HHS Public Access

Author manuscript

Mol Cell Biochem. Author manuscript; available in PMC 2022 March 01.

Published in final edited form as:

Mol Cell Biochem. 2021 March ; 476(3): 1337–1349. doi:10.1007/s11010-020-03993-3.

Deletion of P21 Activated Kinase-1 Induces Age-dependent Increased Visceral Adiposity and Cardiac Dysfunction in Female Mice

Ashley Batra[1], **Chad M. Warren**[1], **Yunbo Ke**[2], **Maximilian McCann**[1], **Monika Halas**[1], **Andrielle E. Capote**[1], **Chong Wee Liew**[1], **R. John Solaro**[1], **Paola C. Rosas**[1,*]

[1]Department of Physiology & Biophysics, Center for Cardiovascular Research, University of Illinois at Chicago, Chicago, IL, United States

[2]Department of Anesthesiology, School of Medicine, University of Maryland, Baltimore, MD, United States

Abstract

It is known that there is an age-related progression in diastolic dysfunction, especially prevalent in post-menopausal women, who develop heart failure with preserved ejection fraction (HFpEF, EF>50%). Mechanisms and therapies are poorly understood, but there are strong correlations between obesity and HFpEF. We have tested the hypothesis that P21 activated kinase-1 (PAK1) preserves cardiac function and adipose tissue homeostasis during aging in female mice. Previous demonstrations in male mice by our lab that PAK1 activity confers cardio-protection against different stresses formed the rationale for this hypothesis. Our studies compared young (3–6 months) and middle-aged (12–15 months) female and male PAK1 knock-out mice ($PAK1^{-/-}$) and wild-type (WT) equivalent. Female WT mice exhibited increased cardiac PAK1 abundance during aging. By echocardiography, compared to young WT female mice, middle-aged WT female mice showed enlargement of the left atrium as well as thickening of posterior wall and increased left ventricular mass; however, all contraction and relaxation parameters were preserved during aging. Compared to WT controls, middle-aged $PAK1^{-/-}$ female mice demonstrated worsening of cardiac function involving a greater enlargement of the left atrium, ventricular hypertrophy and diastolic dysfunction. Moreover, with aging $PAK1^{-/-}$ female mice, unlike male $PAK1^{-/-}$ mice, exhibited increased adiposity with increased accumulation of visceral adipose tissue. Our data provide

*Correspondence: Paola C. Rosas, prosas@uic.edu.

Authors' contributions. AB, MH, AC and CMW performed and analyzed biochemical experiments. MM performed NMR studies. PCR performed and analyzed echocardiography data as well as prepared and wrote the manuscript. YK, CMW, CWL, RJS, and PCR were involved in experimental design, data evaluation analysis and manuscript editing.

DECLARATIONS

Conflicts of interest. R. John Solaro is a member of the Scientist Advisory Board of Cytokinetics, Inc., a consultant for Pfizer, Inc., Edgewise Therapeutics, Inc., and a consultant to Amgen as a member of their Heart Failure Advisory Board. All other authors declare no conflict of interest.

Availability of data and material. Datasets generated for this study are available on request to the corresponding author.

evidence for the significance of PAK1 signaling as an element in the preservation of cardiac function and adipose tissue homeostasis in females during aging.

Keywords

P21 activated kinase-1; aging, females; diastolic dysfunction; heart failure with preserved ejection fraction; obesity; adipose tissue

INTRODUCTION

Heart failure (HF) affects about 6.2 million Americans [8]. HF with preserved ejection fraction (HFpEF), EF>50%, comprises about 50% of all HF diagnoses [9] and continues to lack effective treatment [10,9]. HFpEF occurs in a greater proportion in postmenopausal women vs. men [11–13] and the cause of this difference is unclear. Although multiple upstream pathophysiological etiologies can lead to HFpEF (e.g. aging, hypertension, excess weight), diastolic dysfunction remains a common characteristic of HFpEF [14]. On the other hand, obesity is a global epidemic growing at a fast rate. Over 50% of the world's population [15] and 69% of Americans are either overweight or obese [16]. Moreover, obesity and extreme obesity are higher in women than men (National Center for Health Statistics) and it is a particular concern for women in midlife [17]. Obesity by itself doubles the risk of developing HF [18], and HFpEF is more frequently seen in obese patients (>80% of HFpEF patients are overweight or obese) [19,20].

Novel data reported here support the hypothesis that P21 activated kinase 1 (PAK1) preserves cardiac function and adipose tissue homeostasis in middle-aged female mice. PAK1 is a pleiotropic serine/threonine protein kinase directly activated by Cdc42/Rac1 [5]. Cdc42/Rac1 binding to PAK1 induces a conformational change allowing autophosphorylation and activation [6,7]. Previous studies in male mice in our laboratory reported that PAK1 is a prominent inhibitor of cardiac hypertrophy [1,2], fibrosis [1], maladaptive adrenergic signaling [3] and ROS signaling [4]. Despite these important findings, age-dependent and sex-related comparisons of the role for PAK1 have not been investigated. Data reported here indicate sex related differences are present and may play a role in heart failure progression with aging. Moreover, we discovered that PAK1 is present in the adipose tissue and that lack of PAK1 results in female fat accumulation that accentuates with aging. Our overall hypothesis is that PAK1 regulatory activities in female mice are important to preserve cardiac function and adipose tissue homeostasis. Under certain conditions, this balance may be broken leading to heart failure and obesity. We tested this hypothesis by aging wild type (WT) and global knock-out PAK1 mice ($PAK1^{-/-}$) for 12–15 months to mimic middle-aged humans. Our studies discovered that during aging, WT females exhibit increased PAK1 abundance in the heart which we propose occurs in an attempt to preserve cardiac function. As a proof of concept, disruption of PAK1 signaling in middle-aged $PAK1^{-/-}$ female mice, led to concentric hypertrophy, and diastolic dysfunction. Moreover, middle-aged $PAK1^{-/-}$ female mice exhibited a significant increase of visceral adiposity, like the effects of aging in some women.

MATERIAL AND METHODS

Mouse Lines.

All protocols were approved by the Animal Care and Use Committee of the University of Illinois at Chicago. All animal procedures were conducted in accordance with the Guide for the Care and Use of Laboratory Animals published by the United States National Institutes of Health, Eighth Edition, 2011. Transgenic PAK1 knock-out mice were previously generated in SV129 background [21,22]. The transgenic PAK1 knock-out mice have since been rederived in a FVB/N genetic background, as previously described [3]. In the current study, we used these PAK1 knock-out mice ($PAK1^{-/-}$) in the FVB/N background, young males and females (3–6 months) and old males and females (12–15 months) for acquisition of echocardiography, Western blotting analysis, fat content and organ measurements. Age and sex matched FVB/N mice were used as wild type (WT) controls.

Heart Homogenate Preparation.

Mouse ventricles (10–15mg) were prepared in standard relaxing buffer (SRB: 75 mM KCl, 10 mM Imidiazole pH 7.2, 2 mM MgCl2, 2 mM EGTA, 1 mM NaN3) at a 1:10 ratio relative to tissue weight. All buffers contained protease inhibitors (Sigma, P-8340, St. Louis, MO) and phosphatase inhibitor cocktail (Millipore, 524624, Burlington, MA) at a 1:100 dilutions as well as 100nM Calyculin A (Cell Signaling Technology, 9902, Danvers, MA) solubilized in DMSO. Samples were homogenized at 4°C using the Bead Ruptor 24 Elite Homogenizer (Omni International, 19–040E, Keenesaw, GA) at the following settings: Power: 5 m/s, Time: 15 sec, 3 cycles, 3 minute dwell between each cycle. Homogenized samples were re-suspended with Industrial Sample Buffer (ISB: 8 M urea, 2 M thiourea, 50 mM Tris pH 6.8, 3% SDS, 75 mM DTT, 0.05% bromophenol blue) [24] or 2X Laemmli Sample Buffer (Bio-Rad, Inc., cat#1610737, Hercules, CA) at 1:5 ratio relative to the homogenized protein and vortexed for 15 min. The samples were sonicated in a water bath for 10 min and underwent one freeze/thaw cycle. The samples were heated for 3 min at 100°C then spin clarified at room temperature at 21,000 x G for 3 min. Concentrations were obtained using the Pierce 660 nM Protein Assay with the addition of the IDCR reagent (Thermo Fisher Scientific, 22660, Rockford, IL). Samples were stored at −80°C.

Adipose tissue sample preparation.

Perigonadal mouse tissue (40–50 mg) was prepared in RIPA buffer (Sigma-Aldrich, R0278, St. Louis, MO) at a 1:3 ratio relative to tissue weight in 0.5 ml bead mill tubes with 1.4 mm ceramic beads (Omni International, 19626, Keenesaw, GA). All buffers contained protease inhibitors (Sigma, P-8340, St. Louis, MO) and phosphatase inhibitor cocktail set II (Millipore, 524625, Burlington, MA) and III (Millipore, 524627, Burlington, MA) at a 1:100 dilution. Samples were homogenized at 4°C using the Bead Ruptor 24 Elite Homogenizer (Omni International, 19–040E, Keenesaw, GA) at the following settings: Power: 5 m/s, Time: 30 sec, 1 cycle. The contents were spun down at max speed at 4°C for 10 min, resulting in three layers: a fat layer (top), the supernatant (middle), and the pellet (bottom). The supernatant was removed and was spun down again at max speed at 4°C for 10 min. The second supernatant was extracted and solubilized in 5X Laemmli buffer (50% glycerol, 500 mM DTT, 7.5% SDS, 300 mM Tris base, pH 6.8, 0.1% bromophenol blue) to a 1X

dilution [25]. Protein concentrations were obtained using the Pierce 660 nM Protein Reagent (Thermo Fisher Scientific, 22660, Rockford, IL) with the addition of the IDCR reagent (Thermo Fisher Scientific, 22663, Rockford, IL). Samples were heated for 10 min at 95°C, then stored at −80°C.

Gel Electrophoresis.

Samples were loaded onto a 12% or 15% SDS-PAGE, 0.5% C, pH 8.8 [24]. The gel ran at 200V for 75 minutes in Tris-Glycine running buffer (0.025 M Tris Base, 0.192 M Glycine, 0.1% SDS) in a criterion cell (Biorad Inc., 1656001, Hercules, CA). Phosphorylated variants of cardiac and adipose PAK1 were separated on 8% SDS-PAGE gels containing 50 μM phos-tag (Fujifilm Wako Chemicals, AAL-107, NARD Institute, Ltd. Japan) and 100 μM MnCl2 [26]. Phos-tag gels were run at 20 mA/gel for 75–110 min.

Western Blotting Analysis.

1D SDS-PAGE gels were transferred onto either a 0.2 μm nitrocellulose or polyvinylidene difluoride (PVDF) membrane for 90 min at 20V in a criterion tank blotter (Bio-Rad, Inc., 13036, Hercules, CA). Phos-tag gels were treated twice with 5 mM EDTA in the transfer buffer (10mM CAPS, pH 11.0 [27]) for 10 minutes each time, then washed once with transfer buffer for 10 minutes. The gel was then transferred onto either a 0.2 μm nitrocellulose or 0.2 μm PVDF membrane for 90 min at 30V. To visualize post-transfer efficiency and loading, the blot was stained with SWIFT Stain following manufacturers recommendations (G-Biosciences, 786677, St. Louis, MO). All blots were blocked in either 5% nonfat dry milk+ TBS-T (Tris-buffered saline, pH 7.5, 0.1% Tween-20) or 2% bovine serum albumin (BSA) + TBS-T for 1 hour at room temperature. The blots were washed once with 1X TBS-T prior to addition of the primary antibody. Primary antibodies were incubated overnight at 4°C. All primary and secondary antibodies' dilutions and suppliers are listed in Supplementary Table 1. Three 5-minute washes of 1X TBS-T were done following primary antibody incubation. Secondary antibodies were incubated for 90 minutes at room temperature. Three 5-minute washes of TBS-T were done following secondary incubation. The blots were developed with Clarity ECL Substrate (Bio-Rad, Inc., 1705061, Hercules, CA) or SuperSignal West Femto Maximum Sensitivity ECL Substrate (Thermo Fisher Scientific, 34094, Waltham, MA). ChemiDoc MP Imaging System (Bio-Rad, Inc., Hercules, CA) was used to image gels and blots. Band densities were determined and analyzed using ImageLab 6.0.1 software (Bio-Rad, Inc., Hercules, CA) and Microsoft Excel.

Echocardiography.

Vevo 2100 system (FUJIFILM VisualSonics, Toronto, Ontario, Canada) with MS550 probe 30 um resolution were used to perform echocardiography. We induced anesthesia with 3% isoflurane in 100% O_2 and placed the mouse in echocardiography warming plate to maintain mouse body temperature close to 37°C during the procedure. We maintained anesthesia at 1.5–2.5% throughout the procedure. ECG was continuously monitored. We adjusted the isoflurane concentration to maintain a heart rate in the range of 380–460 beats per minute. We used B-mode to obtain 2-dimenstional real time long axis view images and then changed to M-Mode to obtain images of the left ventricle (LV), aortic root and left atrium (LA). We used the parasternal short axis view at the level of the papillary muscles to measure LV

internal dimension, anterior and posterior wall thickness. Afterwards, we repositioned the stand to the Trendelenburg position and positioned the probe to obtain the apical 4-chamber view. We used color Doppler as a guidance in apical 4-chamber view to obtain blood flow Doppler and measured the peak velocities of flow in early diastole (E) and after LA contraction (A). In this same view we measured tissue Doppler close to the mitral valve annulus at the septal portion and measured peak myocardial relaxation velocity in early diastole (e') and after LA contraction (a') and peak myocardial contraction velocity in systole (s'). All measurements and calculation were averaged from three consecutive cycles. [28]. Data analysis was performed using Vevo Analytic Softwate (VisualSonics, Toronto, ON, Canada).

Total fat mass measurements.

Total fat mass was measured using a Nuclear Magnetic Resonance (TD-NMR Minispec LF50) body composition live mouse analyzer. With NMR technology we were able to analyze fat tissue, lean tissue and free body fluid. Mice were awake and placed in a cylindrical container inside the NMR machine. The procedure took about 2 minutes per mouse. After procedure mice were placed back into their cages.

Adipose Tissue Measurements.

The major fat depots are traditionally classified as white adipose tissue (WAT) and brown adipose tissue (BAT). WAT is comprised by subcutaneous adipose tissue, and visceral adipose tissue. Visceral-WAT surrounds the inner organs and can be divided in mesenteric and perigonadal [29]. Identification and dissection of mouse adipose depots were previously described [30–32]. Briefly, anesthetized mice were placed on a dissection pan. Dorsal and ventral external surfaces of the mouse were sterilized using 70% ethanol. Heart was harvested for biochemistry studies. While having the mouse lay on its back in a supine position, skin and peritoneal cavity wall were cut with a vertical incision. Perigonadal WAT was identified as the WAT that surrounds the uterus and ovaries in females and the WAT that is bound to the epididymis, and testes in males. Mesenteric WAT surrounded the small and large intestines. To dissect this depot, we removed the intestines by cutting at the base of the stomach and the rectum. We used forceps to separate the WAT away from the intestines beginning at the duodenum and continuing to the end of the rectum. To identify subcutaneous WAT, we used forceps to peel back the skin from the peritoneal cavity and the lower limb and found subcutaneous WAT located to the upper site of the hind limbs and underneath the skin. To isolate BAT, mouse was laid in a prone position and dorsal skin was cut. BAT was located between the scapulae. All these fat depots (left and right) were weighted and normalized to tibia length.

Food intake.

Food intake was calculated by weighting the food pellets consumed by single caged mice for an average of 5 days. Food weight was normalized to the body weight of the animal and divided by the number of days the mice were single caged and expressed as food intake index.

Statistical Analysis.

Statistical analysis was performed using GraphPad Prism 8.0.2 Software (GraphPad, Inc., San Diego, CA). Data was analyzed with a two-way ANOVA with Fisher LSD test and multiple comparisons to identify significant differences among 3 or more groups. Student's *t*-test was used to compare 2 independent groups. P values of less than 0.05 were considered statistically significant. Shapiro-Wilks test was used to assess normality, and Spearman's rank correlation test was used to detect heteroscedasticity. Data was presented as mean ± SEM.

RESULTS

PAK1 abundance increased with aging in WT female mice hearts.

Western blot analysis indicated that PAK1 abundance increased in the hearts of middle-aged WT female mice compared to young WT females and to middle-aged WT male mice (Figure 1A, B). Mn^{2+}-Phos-Tag analyses revealed that doubly phosphorylated PAK1 significantly decreased with aging in WT female, but not in male mice (Figure 1C, D). This increased PAK1 abundance in female aging hearts should be considered an important element in the response to aging and as a potential compensatory mechanism to decreased PAK1 phosphorylation.

Phosphorylation levels of Cdc42 increased with aging in WT female mice hearts.

Phosphorylation of Cdc42 at Ser71 significantly increased with aging in female hearts (Figure 2A, B). Previously, it has been reported that phosphorylation of Rac1 and Cdc42 at Ser71 abrogated their binding to their common effector protein, PAK1 [33]. Thus, increased Cdc42 phosphorylation in middle-aged WT female mice would likely result in diminished PAK1 activation. Our results suggest that with aging, WT females develop compensatory mechanisms to preserve cardiac function. These compensatory mechanisms include increased PAK1 abundance in response to decreased Cdc42 activity. No significant differences in Cdc42 abundance were found between groups (Figure 2C, D).

Disruption of PAK1 signaling in middle-aged female mice induced hypertrophy and impaired diastolic function.

In view of our results showing that PAK1 might be a critical signaling pathway that limits cardiac dysfunction in middle-aged female mice, we used echocardiography to study cardiac structure and cardiac function in WT and $PAK1^{-/-}$ mice (Figure 3, and 4, Supplementary Tables 2–4). Figure 3A shows representative M-mode images of short axis and the thickness of the posterior left ventricular (LV) wall during diastole, that is increased in middle-aged $PAK1^{-/-}$ female mice. Tissue Doppler images of the mitral annulus showed that middle-aged $PAK1^{-/-}$ female mice have the slowest peak myocardial relaxation velocity (e') (Figure 3B). All mice maintained an ejection fraction (EF) > 50% (Figure 4A). $PAK1^{-/-}$ males, WT females, and $PAK1^{-/-}$ female hearts showed increased left atrium (LA) diameter with aging (Figure 4B). Both WT and $PAK1^{-/-}$ female hearts showed increased LV posterior wall thickness in diastole (PWd) with aging, but middle-aged $PAK1^{-/-}$ females showed the thickest wall among the other female groups (Figure 4C). $PAK1^{-/-}$ males, WT females, and

PAK1$^{-/-}$ female hearts showed increased LV mass during aging; but both middle-aged PAK1$^{-/-}$ males and PAK1$^{-/-}$ female mice exhibited the highest LV mass among the other groups (Figure 4D). Middle-aged PAK1$^{-/-}$ female hearts showed the highest relative wall thickness (RWT) (Figure 4E), calculated as: (interventricular septum + posterior wall thickness at end-diastole)/(LV internal diameter at end-diastole). Taken together, increased LV wall thickness, increased LV mass and increased RWT suggest that middle-aged PAK1$^{-/-}$ female mice exhibited concentric LV hypertrophy. Additionally, PAK1$^{-/-}$ middle-aged female hearts exhibited slower tissue Doppler of myocardial contraction velocity during systole (s') when compared to WT groups (Figure 4F). Moreover, PAK1$^{-/-}$ aged female hearts exhibited impaired relaxation as shown by the slowest peak myocardial relaxation velocity (e') during early diastolic filling (Figure 3B and 4G), the highest blood flow Doppler (E) to e' ratio (E/e') (Figure 4H), and the longest E wave deceleration time (DT) (Figure 4I). In summary, PAK1$^{-/-}$ female hearts developed concentric LV hypertrophy and deterioration of diastolic function with aging.

PAK1 was present in visceral adipose tissue.

PAK1 was detected by Western blot in perigonadal visceral adipose tissue and its abundance showed a trend for increase in middle-aged WT female mice (Figure 5A, B). No differences were found in the relative ratio of PAK1 phosphorylation forms over total PAK1, detected with Mn^{2+}-Phos-Tag analyses (Figure 5C, D). Additionally, we did not find any changes in Cdc42 abundance in perigonadal visceral adipose tissue (Supplementary Figure 1); however, we were not able to detect by Western blot the phosphorylated form of Cdc42 in adipose tissue.

Deletion of PAK1 caused increased visceral adiposity in middle-aged female mice.

When aged, PAK1$^{-/-}$ females exhibited a significant increase in body weight reaching similar levels to aged PAK1$^{-/-}$ male mice on a standard chow diet (Figure 6A). Moreover, middle-aged PAK1$^{-/-}$ female mice showed the highest percentage of fat mass assessed by Nuclear Magnetic Resonance (Figure 6B) and the greatest accumulation of visceral WAT, including perigonadal (Figure 6C) and mesenteric fat (Figure 6D). Sub-cutaneous fat was also higher in middle-aged PAK1$^{-/-}$ females compared to the other female groups; however, no differences were found between middle-aged PAK1$^{-/-}$ males and females (Figure 6E). As shown in Figure 6F, there were similar levels of brown adipose tissue (BAT) regardless of sex, age, or expression of PAK1. We did not find any differences in food intake between groups (Figure 6G); thus, increased fat accumulation in middle-aged PAK1$^{-/-}$ female mice cannot be attributed to increased food intake.

DISCUSSION

In this study we have identified a novel protective role of PAK1 in response to aging in female mice. Our major findings are: 1) PAK1 is more abundant in middle-aged WT female mice hearts in response to decreased Cdc42 activity; 2) PAK1 is present in visceral adipose tissue; and 3) Global deletion of PAK1 results in obesity, concentric cardiac hypertrophy and diastolic dysfunction in middle-aged female mice only.

Preservation of cardiac function during aging in WT female mice is likely due to increased PAK1 abundance.

This is the first study to demonstrate that PAK1 abundance in the heart differs between males and females during aging. Lack of PAK1, in middle-aged female mice, results in hypertrophy and impaired diastolic function (Figure 3 and 4). Previous reported studies employing a conditional cardiac tissue specific PAK1 knock-out mouse model ($PAK1^{cko}$) demonstrated that the absence of PAK1 exacerbates cardiac hypertrophy in a pressure overload mouse model. In this same study, FTY720 a PAK1 activator, prevented pressure overload-induced hypertrophy [2]. However, these studies only used $PAK1^{cko}$ male mice. The lack of PAK1 in female hearts was not addressed. Moreover, the participation of PAK1 in the response to aging has not been investigated. Clinical research has demonstrated that premenopausal females have lower risk of developing heart failure compared to men at the same age; however, this advantage is lost after entering menopause, when the rate of cardiac hypertrophy and diastolic dysfunction significantly increase among postmenopausal women [34,35]. Studies in aged rat models showed that the absence of estrogens induced diastolic dysfunction with preserved ejection fraction [36]. Furthermore, there is evidence in other tissues that PAK1 is regulated by estrogens through estrogen receptor-α (ERα) [37]; thus, it is possible that a decline of estrogen signaling in the hearts of our 12–15 month-old WT female mice, as it was previously shown in other organs [38–40], triggers a compensatory increase in PAK1 abundance as a cardio-protective mechanism against aging. However, under certain conditions these mechanisms may be altered and may result in overt heart failure. In future studies, it will be of interest to determine the abundance and phosphorylation of PAK1 in the hearts of pre and postmenopausal women with and without heart failure, to corroborate our hypothesis. It may be possible that women that cannot compensate aging with increased cardiac PAK1 levels will be more prone to hypertrophy and diastolic dysfunction, as seen in our middle-aged female $PAK1^{-/-}$ mice. On the other hand, males seem to use other compensatory mechanisms to preserve cardiac function during aging, different from females and that may be hormone related.

Downregulation of Cdc42 in middle-aged WT female mice hearts triggers a compensatory increase in PAK1 abundance.

In the present study, our data indicated that with aging WT female hearts showed an increase in phosphorylated levels of Cdc42 (pSer-71) (Figure 2A, B), likely to induce a decrease in Cdc42 activity. Interactions with PAK1 were abrogated by pseudo-phosphorylation (S71E) of Cdc42 and Rac1 [33], thereby negatively affecting their activity. Furthermore, using a cardiac specific deletion of Cdc42 mouse model, it was demonstrated that Cdc42 acts as an antihypertrophic mediator in mice hearts [41]. Conversely, others have shown that overexpression of Cdc42 enhances myocyte growth in culture, whereas overexpression of a dominant-negative Cdc42 mutant reduced cardiomyocyte growth [42]. We propose that increased PAK1 abundance in middle-aged $PAK1^{-/-}$ female mice (Figure 1A, B) provides a compensatory mechanism in response to decreased Cdc42 upstream activity. It is of interest that all $PAK1^{-/-}$ mice groups show overall decreased levels of Cdc42 phosphorylation, that may be due to a lack of regulatory feedback from PAK1 (Supplementary Figure 2A, B).

With aging female PAK1$^{-/-}$ mice show impaired myocardial relaxation not present in WT females.

Echocardiography data showed concentric hypertrophy in middle-aged PAK1$^{-/-}$ female mice as indicated by increased posterior ventricular wall thickness (Figure 3A and 4C), increased LV mass (Figure 4D) and increased RWT (Figure 4E). In humans, concentric hypertrophy is defined as increased LV index (LV mass normalized to body surface area) and RWT greater than 0.42 [44]. For our echocardiographic analyses in mice, we used the corrected LV mass value, as calculated by Vevo LAB software, and the RWT formula: (interventricular septum + posterior wall thickness)/(LV internal diameter at end-diastole). Even though the RWT values in the middle-aged PAK1$^{-/-}$ female mice group did not reach human levels of >0.42, RWT in this group of mice was the highest and significantly different from the other female groups. Middle-aged PAK1$^{-/-}$ females also showed left atrial enlargement (Figure 4B) that in humans is frequently correlated to left ventricular hypertrophy, diastolic dysfunction, and atrial fibrillation [46,47]. Moreover, middle-aged PAK1$^{-/-}$ females exhibited slower peak myocardial relaxation velocity, e' (Figure 4G), higher E/e' ratios (Figure 4H) and prolonged E wave deceleration time (Figure 4I) that together with an EF≥50% resemble human HFpEF with compromised diastolic function and LV hypertrophy [48]. Even though, middle-aged WT females also exhibited left atrial enlargement, posterior wall thickening and increased LV mass during aging, these were to a lesser degree than middle-aged PAK1$^{-/-}$ females (Figure 4B–D). Interestingly, middle-aged WT females maintain a constant e' (Figure 4G), E/e' (Figure 4H) and E wave deceleration time with aging (Figure 4I); suggesting that increased PAK1 abundance in this group of mice prevents impaired relaxation. On the other hand, middle-aged PAK1$^{-/-}$ males also showed left atrial enlargement (Figure 4B), higher LV mass (Figure 4D), and slower e' (Figure 4G); however, all the other contraction and relaxation parameters (i.e. s', E/e', DT) remained constant and did not differ between male groups. Thus, regulatory mechanisms that govern aging adaptation appear to be depend on PAK1 abundance and to differ between males and females.

Middle-aged PAK1$^{-/-}$ female mice exhibit increased visceral white adipose tissue mass.

Our studies show, for the first time, that PAK1 is present in adipose tissue (Figure 5A, B) and that deletion of PAK1 affects adipose tissue homeostasis. Middle-aged PAK1$^{-/-}$ male and female mice exhibited increased body weight when compared to the other groups (Figure 6A). However, middle-aged PAK1$^{-/-}$ female mice show the highest percentage of fat mass assessed by NMR (Figure 6B) with the greatest accumulation of perigonadal visceral fat (Figure 6C) and mesenteric fat (Figure 6D). Interestingly, there were no differences in food intake between groups (Figure 6G); thus, the increased adiposity observed in the middle-aged PAK1$^{-/-}$ female group, cannot be attributed to increased food intake. It was previously reported that PAK1 activates protein phosphatase 2A (PP2A) in the heart [51]. PP2A is an important and ubiquitously expressed serine threonine phosphatase [52] that may also be involved in the dephosphorylation of important regulatory proteins in the adipocytes. Moreover, it was shown that PPARγ, a key regulatory protein for adipogenesis, is downregulated by PAK1 in a setting of intestinal inflammation [53]. Thus, it is highly possible that PAK1, through PP2A, regulates the phosphorylation of PPARγ and other

adipose tissue regulatory proteins to act as an inhibitory kinase for adiposity. Future studies will explore these novel regulatory pathways that involve PAK1 in adipose tissue regulation.

Figure 7 illustrates our hypothesis related to increased levels of PAK1 in middle-aged WT female mice. Aging in females, may promote GPCR (G-protein-coupled receptor) activation, increased levels of adenylyl cyclase and PKA activation [54] with the consequent phosphorylation and inactivation of Cdc42. It was previously shown that PKA phosphorylation of Rho small GTPases, such as Cdc42 and RhoA, significantly increased their interaction with GDI (guanine nucleotide dissociation inhibitor) forming inactive complexes that translocate from the plasma membrane to the cytosol [55]. Moreover, phosphorylation of Cdc42 inhibits its binding to PAK1 [33]. Thus, as a compensatory mechanism in response to the reduction in Cdc42 activity, middle-aged WT females may increase the abundance of PAK1. This increase in PAK1 abundance may be an important protective mechanism in various organs such as the adipose tissue and the heart (Figure 7A). This may also be a common mechanism that explains both the higher incidence of obesity and HF in postmenopausal women that occurs when the compensatory increased abundance of PAK1 is not achieved (Figure 7B).

CONCLUSION

Our study provides a novel, first line of evidence that PAK1 is an important pathway to preserve cardiac function and adipose tissue homeostasis in females during aging. Deletion of PAK1 leads to cardiac hypertrophy, diastolic dysfunction and obesity as female mice grow to middle-age. These findings set the stage for investigation of the downstream signaling mechanisms of PAK1 in the female heart and the adipose tissue and the downstream signals affected with aging by PAK1 deletion. Our data also indicate that increased PAK1 abundance may be a general mechanism of preservation of function in females during aging. Given that PAK1 is localized in various organs, an overall decrease in PAK1 activity due to pathological conditions will deleteriously affect their function. Here we focused on the heart and the adipose tissue, which were the more evident organs affected in our middle-aged female mice with global PAK1 deletion; however, other organs may also be affected. To dissect the effects of PAK1 deletion in the heart and in the adipose tissue, separately, we will create cardiac tissue-specific and adipose tissue-specific PAK1 knock-out mouse models. This approach will also serve to investigate how obesity, expected to be observed in the adipose tissue-specific PAK1 knock-out model, affects cardiac function.

Supplementary Material

Refer to Web version on PubMed Central for supplementary material.

Acknowledgments

Funding. Our work was supported by NIH grants P01 HL062426 Project 1 (RJS) and Core C (CMW), 3P01HL062426-18S1 (PCR) and 1R25HL145817-01 (PCR).

REFERENCES

1. Liu W, Zi M, Tsui H, Chowdhury SK, Zeef L, Meng QJ, Travis M, Prehar S, Berry A, Hanley NA, Neyses L, Xiao RP, Oceandy D, Ke Y, Solaro RJ, Cartwright EJ, Lei M, Wang X (2013) A novel immunomodulator, FTY-720 reverses existing cardiac hypertrophy and fibrosis from pressure overload by targeting NFAT (nuclear factor of activated T-cells) signaling and periostin. Circ Heart Fail 6 (4):833–844. doi:10.1161/CIRCHEARTFAILURE.112.000123 [PubMed: 23753531]
2. Liu W, Zi M, Naumann R, Ulm S, Jin J, Taglieri DM, Prehar S, Gui J, Tsui H, Xiao RP, Neyses L, Solaro RJ, Ke Y, Cartwright EJ, Lei M, Wang X (2011) Pak1 as a novel therapeutic target for antihypertrophic treatment in the heart. Circulation 124 (24):2702–2715. doi:10.1161/CIRCULATIONAHA.111.048785 [PubMed: 22082674]
3. Taglieri DM, Monasky MM, Knezevic I, Sheehan KA, Lei M, Wang X, Chernoff J, Wolska BM, Ke Y, Solaro RJ (2011) Ablation of p21-activated kinase-1 in mice promotes isoproterenol-induced cardiac hypertrophy in association with activation of Erk1/2 and inhibition of protein phosphatase 2A. J Mol Cell Cardiol 51 (6):988–996. doi:10.1016/j.yjmcc.2011.09.016 [PubMed: 21971074]
4. DeSantiago J, Bare DJ, Xiao L, Ke Y, Solaro RJ, Banach K (2014) p21-Activated kinase1 (Pak1) is a negative regulator of NADPH-oxidase 2 in ventricular myocytes. J Mol Cell Cardiol 67:77–85. doi:10.1016/j.yjmcc.2013.12.017 [PubMed: 24380729]
5. Manser E, Leung T, Salihuddin H, Zhao ZS, Lim L (1994) A brain serine/threonine protein kinase activated by Cdc42 and Rac1. Nature 367 (6458):40–46 [PubMed: 8107774]
6. Lei M, Robinson MA, Harrison SC (2005) The active conformation of the PAK1 kinase domain. Structure 13 (5):769–778. doi:10.1016/j.str.2005.03.007 [PubMed: 15893667]
7. Strochlic TI, Viaud J, Rennefahrt UE, Anastassiadis T, Peterson JR (2010) Phosphoinositides are essential coactivators for p21-activated kinase 1. Mol Cell 40 (3):493–500. doi:10.1016/j.molcel.2010.10.015 [PubMed: 21070974]
8. Benjamin EJ, Muntner P, Alonso A, Bittencourt MS, Callaway CW, Carson AP, Chamberlain AM, Chang AR, Cheng S, Das SR, Delling FN, Djousse L, Elkind MSV, Ferguson JF, Fornage M, Jordan LC, Khan SS, Kissela BM, Knutson KL, Kwan TW, Lackland DT, Lewis TT, Lichtman JH, Longenecker CT, Loop MS, Lutsey PL, Martin SS, Matsushita K, Moran AE, Mussolino ME, O'Flaherty M, Pandey A, Perak AM, Rosamond WD, Roth GA, Sampson UKA, Satou GM, Schroeder EB, Shah SH, Spartano NL, Stokes A, Tirschwell DL, Tsao CW, Turakhia MP, VanWagner LB, Wilkins JT, Wong SS, Virani SS, American Heart Association Council on E, Prevention Statistics C, Stroke Statistics S (2019) Heart Disease and Stroke Statistics-2019 Update: A Report From the American Heart Association. Circulation 139 (10):e56–e528. doi:10.1161/CIR.0000000000000659 [PubMed: 30700139]
9. Yancy CW, Jessup M, Bozkurt B, Butler J, Casey DE Jr., Drazner MH, Fonarow GC, Geraci SA, Horwich T, Januzzi JL, Johnson MR, Kasper EK, Levy WC, Masoudi FA, McBride PE, McMurray JJ, Mitchell JE, Peterson PN, Riegel B, Sam F, Stevenson LW, Tang WH, Tsai EJ, Wilkoff BL (2013) 2013 ACCF/AHA Guideline for the Management of Heart Failure: A Report of the American College of Cardiology Foundation/American Heart Association Task Force on Practice Guidelines. Circulation. doi:CIR.0b013e31829e8776 [pii] 10.1161/CIR.0b013e31829e8776
10. Yancy CW, Jessup M, Bozkurt B, Butler J, Casey DE Jr., Colvin MM, Drazner MH, Filippatos GS, Fonarow GC, Givertz MM, Hollenberg SM, Lindenfeld J, Masoudi FA, McBride PE, Peterson PN, Stevenson LW, Westlake C (2017) 2017 ACC/AHA/HFSA Focused Update of the 2013 ACCF/AHA Guideline for the Management of Heart Failure: A Report of the American College of Cardiology/American Heart Association Task Force on Clinical Practice Guidelines and the Heart Failure Society of America. Circulation 136 (6):e137–e161. doi:10.1161/CIR.0000000000000509 [PubMed: 28455343]
11. Lam CS, Donal E, Kraigher-Krainer E, Vasan RS (2011) Epidemiology and clinical course of heart failure with preserved ejection fraction. Eur J Heart Fail 13 (1):18–28. doi:10.1093/eurjhf/hfq121 [PubMed: 20685685]
12. Ho JE, Gona P, Pencina MJ, Tu JV, Austin PC, Vasan RS, Kannel WB, D'Agostino RB, Lee DS, Levy D (2012) Discriminating clinical features of heart failure with preserved vs. reduced ejection fraction in the community. Eur Heart J 33 (14):1734–1741. doi:10.1093/eurheartj/ehs070 [PubMed: 22507977]

13. Kane AE, Howlett SE (2018) Differences in Cardiovascular Aging in Men and Women. Adv Exp Med Biol 1065:389–411. doi:10.1007/978-3-319-77932-4_25 [PubMed: 30051398]
14. Kane GC, Karon BL, Mahoney DW, Redfield MM, Roger VL, Burnett JC Jr., Jacobsen SJ, Rodeheffer RJ (2011) Progression of left ventricular diastolic dysfunction and risk of heart failure. JAMA 306 (8):856–863. doi:306/8/856 [pii] 10.1001/jama.2011.1201 [PubMed: 21862747]
15. Kelly T, Yang W, Chen CS, Reynolds K, He J (2008) Global burden of obesity in 2005 and projections to 2030. Int J Obes (Lond) 32 (9):1431–1437. doi:10.1038/ijo.2008.102 [PubMed: 18607383]
16. Flegal KM, Carroll MD, Kit BK, Ogden CL (2012) Prevalence of obesity and trends in the distribution of body mass index among US adults, 1999–2010. JAMA 307 (5):491–497. doi:10.1001/jama.2012.39 [PubMed: 22253363]
17. Flegal KM, Carroll MD, Ogden CL, Curtin LR (2010) Prevalence and trends in obesity among US adults, 1999–2008. JAMA 303 (3):235–241. doi:10.1001/jama.2009.2014 [PubMed: 20071471]
18. Kenchaiah S, Evans JC, Levy D, Wilson PW, Benjamin EJ, Larson MG, Kannel WB, Vasan RS (2002) Obesity and the risk of heart failure. N Engl J Med 347 (5):305–313. doi:10.1056/NEJMoa020245 [PubMed: 12151467]
19. Haass M, Kitzman DW, Anand IS, Miller A, Zile MR, Massie BM, Carson PE (2011) Body mass index and adverse cardiovascular outcomes in heart failure patients with preserved ejection fraction: results from the Irbesartan in Heart Failure with Preserved Ejection Fraction (I-PRESERVE) trial. Circ Heart Fail 4 (3):324–331. doi:10.1161/CIRCHEARTFAILURE.110.959890 [PubMed: 21350053]
20. Shah SJ, Heitner JF, Sweitzer NK, Anand IS, Kim HY, Harty B, Boineau R, Clausell N, Desai AS, Diaz R, Fleg JL, Gordeev I, Lewis EF, Markov V, O'Meara E, Kobulia B, Shaburishvili T, Solomon SD, Pitt B, Pfeffer MA, Li R (2013) Baseline characteristics of patients in the treatment of preserved cardiac function heart failure with an aldosterone antagonist trial. Circ Heart Fail 6 (2):184–192. doi:10.1161/CIRCHEARTFAILURE.112.972794 [PubMed: 23258572]
21. Smith SD, Jaffer ZM, Chernoff J, Ridley AJ (2008) PAK1-mediated activation of ERK1/2 regulates lamellipodial dynamics. J Cell Sci 121 (Pt 22):3729–3736. doi:10.1242/jcs.027680 [PubMed: 18940914]
22. McDaniel AS, Allen JD, Park SJ, Jaffer ZM, Michels EG, Burgin SJ, Chen S, Bessler WK, Hofmann C, Ingram DA, Chernoff J, Clapp DW (2008) Pak1 regulates multiple c-Kit mediated Ras-MAPK gain-in-function phenotypes in Nf1+/− mast cells. Blood 112 (12):4646–4654. doi:10.1182/blood-2008-04-155085 [PubMed: 18768391]
23. Solaro RJ, Pang DC, Briggs FN (1971) The purification of cardiac myofibrils with Triton X-100. Biochim Biophys Acta 245 (1):259–262. doi:0005-2728(71)90033-8 [pii] [PubMed: 4332100]
24. Fritz JD, Swartz DR, Greaser ML (1989) Factors affecting polyacrylamide gel electrophoresis and electroblotting of high-molecular-weight myofibrillar proteins. Anal Biochem 180 (2):205–210 [PubMed: 2817350]
25. Qiang G, Whang Kong H, Xu S, Pham HA, Parlee SD, Burr AA, Gil V, Pang J, Hughes A, Gu X, Fantuzzi G, MacDougald OA, Liew CW (2016) Lipodystrophy and severe metabolic dysfunction in mice with adipose tissue-specific insulin receptor ablation. Mol Metab 5 (7):480–490. doi:10.1016/j.molmet.2016.05.005 [PubMed: 27408774]
26. Kinoshita E, Kinoshita-Kikuta E, Takiyama K, Koike T (2006) Phosphate-binding tag, a new tool to visualize phosphorylated proteins. Mol Cell Proteomics 5 (4):749–757. doi:10.1074/mcp.T500024-MCP200 [PubMed: 16340016]
27. Matsudaira P (1987) Sequence from picomole quantities of proteins electroblotted onto polyvinylidene difluoride membranes. J Biol Chem 262 (21):10035–10038 [PubMed: 3611052]
28. Rosas PC, Warren CM, Creed HA, Trzeciakowski JP, Solaro RJ, Tong CW (2019) Cardiac Myosin Binding Protein-C Phosphorylation Mitigates Age-Related Cardiac Dysfunction: Hope for Better Aging? JACC Basic Transl Sci 4 (7):817–830. doi:10.1016/j.jacbts.2019.06.003 [PubMed: 31998850]
29. Park A, Kim WK, Bae KH (2014) Distinction of white, beige and brown adipocytes derived from mesenchymal stem cells. World J Stem Cells 6 (1):33–42. doi:10.4252/wjsc.v6.i1.33 [PubMed: 24567786]

30. Bagchi DP, MacDougald OA (2019) Identification and Dissection of Diverse Mouse Adipose Depots. J Vis Exp (149). doi:10.3791/59499

31. Mann A, Thompson A, Robbins N, Blomkalns AL (2014) Localization, identification, and excision of murine adipose depots. J Vis Exp (94). doi:10.3791/52174

32. Casteilla L, Penicaud L, Cousin B, Calise D (2008) Choosing an adipose tissue depot for sampling: factors in selection and depot specificity. Methods Mol Biol 456:23–38. doi:10.1007/978-1-59745-245-8_2 [PubMed: 18516550]

33. Schwarz J, Proff J, Havemeier A, Ladwein M, Rottner K, Barlag B, Pich A, Tatge H, Just I, Gerhard R (2012) Serine-71 phosphorylation of Rac1 modulates downstream signaling. PLoS One 7 (9):e44358. doi:10.1371/journal.pone.0044358 [PubMed: 22970203]

34. Regitz-Zagrosek V, Oertelt-Prigione S, Seeland U, Hetzer R (2010) Sex and gender differences in myocardial hypertrophy and heart failure. Circ J 74 (7):1265–1273. doi:10.1253/circj.cj-10-0196 [PubMed: 20558892]

35. Maslov PZ, Kim JK, Argulian E, Ahmadi A, Narula N, Singh M, Bax J, Narula J (2019) Is Cardiac Diastolic Dysfunction a Part of Post-Menopausal Syndrome? JACC Heart failure 7 (3):192–203. doi:10.1016/j.jchf.2018.12.018 [PubMed: 30819374]

36. Bustamante M, Garate-Carrillo A, B RI, Garcia R, Carson N, Ceballos G, Ramirez-Sanchez I, Omens J, Villarreal F (2019) Unmasking of oestrogen-dependent changes in left ventricular structure and function in aged female rats: a potential model for pre-heart failure with preserved ejection fraction. J Physiol 597 (7):1805–1817. doi:10.1113/JP277479 [PubMed: 30681142]

37. Zhao Z, Park C, McDevitt MA, Glidewell-Kenney C, Chambon P, Weiss J, Jameson JL, Levine JE (2009) p21-Activated kinase mediates rapid estradiol-negative feedback actions in the reproductive axis. Proc Natl Acad Sci U S A 106 (17):7221–7226. doi:10.1073/pnas.0812597106 [PubMed: 19359483]

38. Bergman MD, Karelus K, Felicio LS, Nelson JF (1991) Age-related alterations in estrogen receptor dynamics are independent of cycling status in middle-aged C57BL/6J mice. J Steroid Biochem Mol Biol 38 (2):127–133. doi:10.1016/0960-0760(91)90117-n [PubMed: 2004035]

39. Chakraborty TR, Ng L, Gore AC (2003) Age-related changes in estrogen receptor beta in rat hypothalamus: a quantitative analysis. Endocrinology 144 (9):4164–4171. doi:10.1210/en.2003-0052 [PubMed: 12933691]

40. Motohashi R, Takumida M, Shimizu A, Konomi U, Fujita K, Hirakawa K, Suzuki M, Anniko M (2010) Effects of age and sex on the expression of estrogen receptor alpha and beta in the mouse inner ear. Acta Otolaryngol 130 (2):204–214. doi:10.3109/00016480903016570 [PubMed: 19479455]

41. Maillet M, Lynch JM, Sanna B, York AJ, Zheng Y, Molkentin JD (2009) Cdc42 is an antihypertrophic molecular switch in the mouse heart. J Clin Invest 119 (10):3079–3088. doi:10.1172/JCI37694 [PubMed: 19741299]

42. Nagai T, Tanaka-Ishikawa M, Aikawa R, Ishihara H, Zhu W, Yazaki Y, Nagai R, Komuro I (2003) Cdc42 plays a critical role in assembly of sarcomere units in series of cardiac myocytes. Biochem Biophys Res Commun 305 (4):806–810. doi:10.1016/s0006-291x(03)00838-6 [PubMed: 12767901]

43. Azios NG, Krishnamoorthy L, Harris M, Cubano LA, Cammer M, Dharmawardhane SF (2007) Estrogen and resveratrol regulate Rac and Cdc42 signaling to the actin cytoskeleton of metastatic breast cancer cells. Neoplasia 9 (2):147–158. doi:10.1593/neo.06778 [PubMed: 17356711]

44. Lang RM, Badano LP, Mor-Avi V, Afilalo J, Armstrong A, Ernande L, Flachskampf FA, Foster E, Goldstein SA, Kuznetsova T, Lancellotti P, Muraru D, Picard MH, Rietzschel ER, Rudski L, Spencer KT, Tsang W, Voigt JU (2015) Recommendations for cardiac chamber quantification by echocardiography in adults: an update from the American Society of Echocardiography and the European Association of Cardiovascular Imaging. J Am Soc Echocardiogr 28 (1):1–39 e14. doi:10.1016/j.echo.2014.10.003 [PubMed: 25559473]

45. Nagueh SF, Smiseth OA, Appleton CP, Byrd BF 3rd, Dokainish H, Edvardsen T, Flachskampf FA, Gillebert TC, Klein AL, Lancellotti P, Marino P, Oh JK, Alexandru Popescu B, Waggoner AD, Houston T, Oslo N, Phoenix A, Nashville T, Hamilton OC, Uppsala S, Ghent Liege B, Cleveland O, Novara I, Rochester M, Bucharest R, St. Louis M (2016) Recommendations for the Evaluation of Left Ventricular Diastolic Function by Echocardiography: An Update from the American

Society of Echocardiography and the European Association of Cardiovascular Imaging. Eur Heart J Cardiovasc Imaging 17 (12):1321–1360. doi:10.1093/ehjci/jew082 [PubMed: 27422899]

46. Cuspidi C, Negri F, Sala C, Valerio C, Mancia G (2012) Association of left atrial enlargement with left ventricular hypertrophy and diastolic dysfunction: a tissue Doppler study in echocardiographic practice. Blood Press 21 (1):24–30. doi:10.3109/08037051.2011.618262 [PubMed: 21992028]
47. Seko Y, Kato T, Haruna T, Izumi T, Miyamoto S, Nakane E, Inoko M (2018) Association between atrial fibrillation, atrial enlargement, and left ventricular geometric remodeling. Sci Rep 8 (1):6366. doi:10.1038/s41598-018-24875-1 [PubMed: 29686287]
48. Zile MR, Gottdiener JS, Hetzel SJ, McMurray JJ, Komajda M, McKelvie R, Baicu CF, Massie BM, Carson PE, Investigators IP (2011) Prevalence and significance of alterations in cardiac structure and function in patients with heart failure and a preserved ejection fraction. Circulation 124 (23):2491–2501. doi:10.1161/CIRCULATIONAHA.110.011031 [PubMed: 22064591]
49. Gokce M, Karahan B, Erdol C, Kasap H, Ozdemirci S (2003) Left ventricular diastolic function assessment by tissue Doppler echocardiography in relation to hormonal replacement therapy in postmenopausal women with diastolic dysfunction. American journal of therapeutics 10 (2):104–111 [PubMed: 12629588]
50. Voutilainen S, Hippelainen M, Hulkko S, Karppinen K, Ventila M, Kupari M (1993) Left ventricular diastolic function by Doppler echocardiography in relation to hormonal replacement therapy in healthy postmenopausal women. Am J Cardiol 71 (7):614–617. doi:10.1016/0002-9149(93)90525-h [PubMed: 8438755]
51. Ke Y, Wang L, Pyle WG, de Tombe PP, Solaro RJ (2004) Intracellular localization and functional effects of P21-activated kinase-1 (Pak1) in cardiac myocytes. Circ Res 94 (2):194–200. doi:10.1161/01.RES.0000111522.02730.56 [PubMed: 14670848]
52. Ruediger R, Van Wart Hood JE, Mumby M, Walter G (1991) Constant expression and activity of protein phosphatase 2A in synchronized cells. Molecular and cellular biology 11 (8):4282–4285. doi:10.1128/mcb.11.8.4282 [PubMed: 1649390]
53. Dammann K, Khare V, Lang M, Claudel T, Harpain F, Granofszky N, Evstatiev R, Williams JM, Pritchard DM, Watson A, Gasche C (2015) PAK1 modulates a PPARgamma/NF-kappaB cascade in intestinal inflammation. Biochim Biophys Acta 1853 (10 Pt A):2349–2360. doi:10.1016/j.bbamcr.2015.05.031 [PubMed: 26036343]
54. Parks RJ, Bogachev O, Mackasey M, Ray G, Rose RA, Howlett SE (2017) The impact of ovariectomy on cardiac excitation-contraction coupling is mediated through cAMP/PKA-dependent mechanisms. J Mol Cell Cardiol 111:51–60. doi:10.1016/j.yjmcc.2017.07.118 [PubMed: 28778766]
55. Forget MA, Desrosiers RR, Gingras D, Beliveau R (2002) Phosphorylation states of Cdc42 and RhoA regulate their interactions with Rho GDP dissociation inhibitor and their extraction from biological membranes. Biochem J 361 (Pt 2):243–254. doi:10.1042/0264-6021:3610243 [PubMed: 11772396]

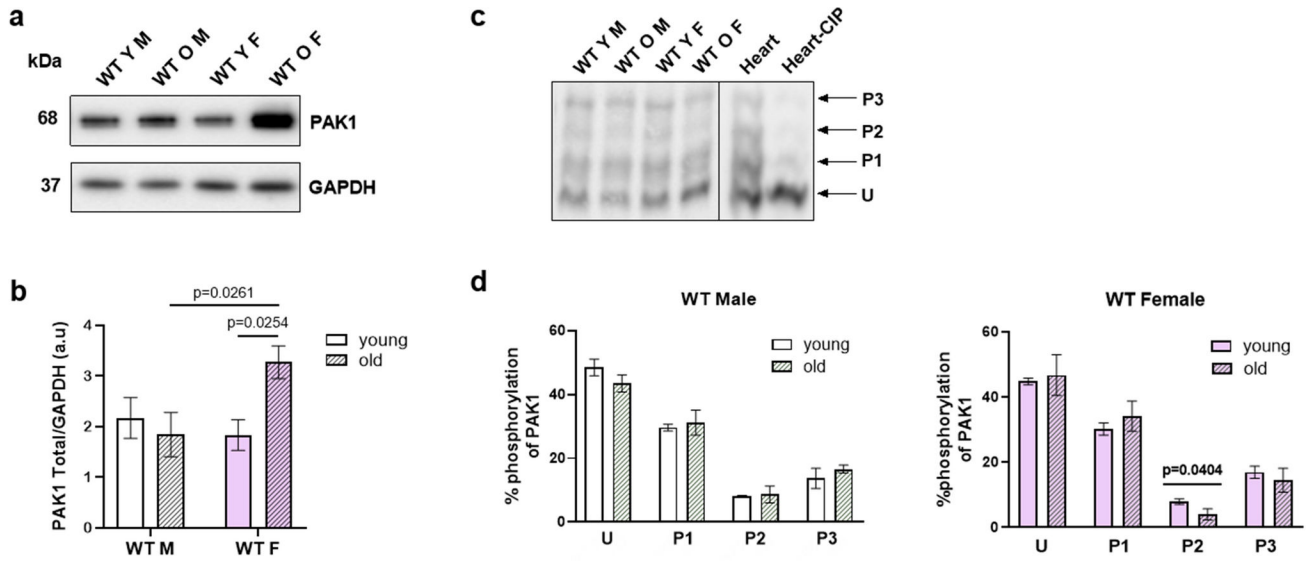

Fig. 1. Wild type (WT) middle-aged female mice hearts exhibited increased PAK1 abundance

(A) Total PAK1 abundance and GAPDH as loading control were detected by Western blot on whole homogenates prepared from hearts. **(B)** Quantification of PAK1 over GAPDH showed PAK1 abundance increased with aging in the hearts of WT female mice. **(C)** PAK1 phosphovariants were separated on an 8% SDS-PAGE phos-tag gel. The bottom band is un-phosphorylated PAK1 (U). The bands above are phosphorylated PAK1 with 1 phosphate group (P1), 2 phosphate groups (P2), and 3 phosphate groups (P3), respectively. To verify that such bands were phosphorylated PAK1, a WT heart was treated with calf intestine phosphatase (CIP). **(D)** Percentage of phosphorylation of each PAK1 band was calculated as p-PAK1/Total PAK1 (total PAK1=unphosphorylated + phosphorylated forms). Doubly phosphorylated PAK1 was decreased in 12–15 months-old female mice when compared to the younger counterpart. Young: 3–6 months, old: 12–15 months. Data presented as mean ± SEM. n=3. Total PAK1 abundance was analyzed with two-way ANOVA Fisher LSD test. PAK1 phosphorylation was analyzed with *t*-test for young vs. old groups.

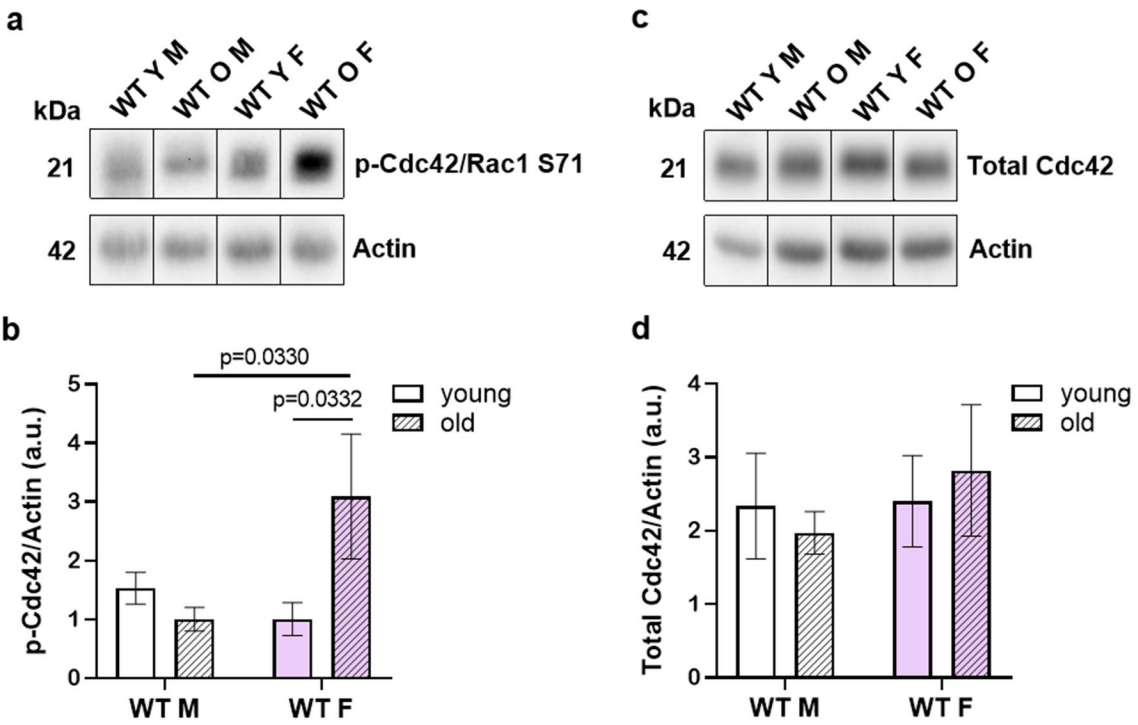

Fig. 2. Phosphorylation of Cdc42 was increased in middle-aged wild type (WT) females' hearts

(A) Phosphorylation of Cdc42 at Ser71, and actin as loading control were detected by Western blot on whole homogenates prepared from hearts. **(B)** Quantification of Cdc42 phosphorylation at Ser71 over actin showed increased phospho levels in middle-aged WT female mice. **(C)** In a separate blot, total Cdc42 abundance, and actin as loading control were detected. **(D)** Total protein levels of Cdc42 over actin remain unchanged. Young: 3–6 months, old: 12–15 months. Data presented as mean ± SEM. n=3. Data was analyzed using two-way ANOVA Fisher LSD test.

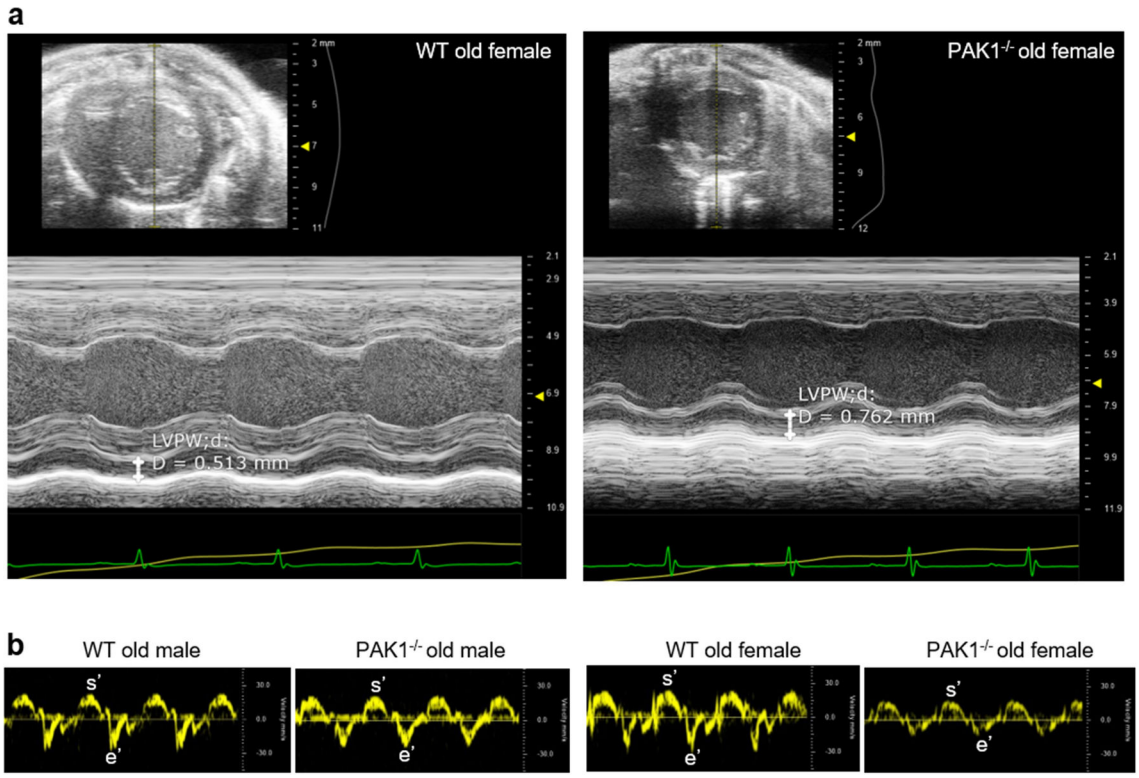

Fig. 3. Echocardiographic measurements showed ventricular hypertrophy and slower myocardial relaxation velocity in middle-aged PAK1$^{-/-}$ female mice

(A) Representative short axis M-mode images of the left ventricle of 12–15 months female WT and PAK1$^{-/-}$ mice. **(B)** Sample tissue Doppler traces of female and male WT and PAK1$^{-/-}$ old mice (12–15 months).

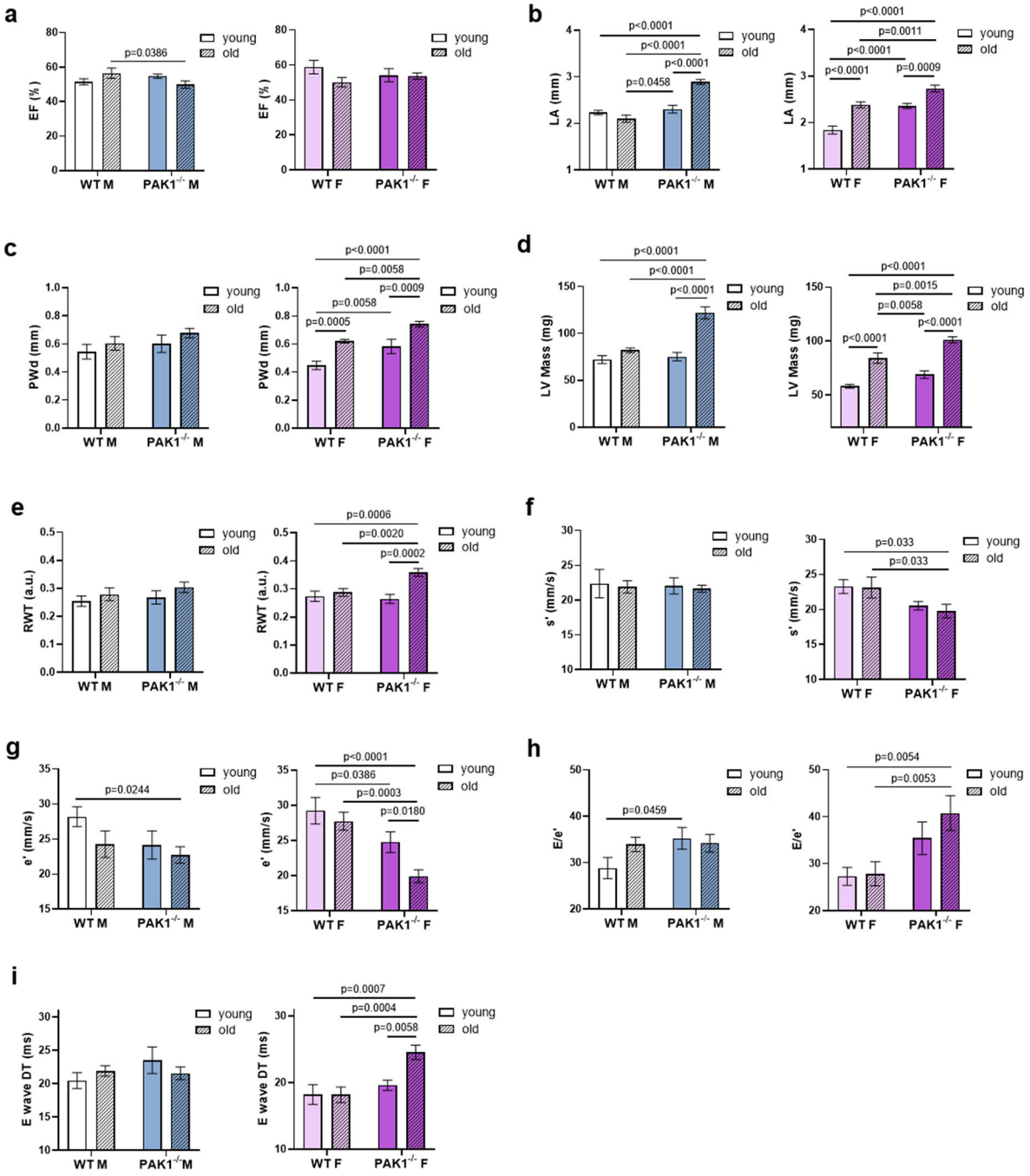

Fig. 4. Middle-aged PAK1$^{-/-}$ female mice demonstrated impaired diastolic function

(A) All mice showed ejection fraction (EF) ≥ 50%. **(B)** Both aged PAK1$^{-/-}$ males and females had enlarged left atrium (LA). **(C)** Female WT and female PAK1$^{-/-}$ mice showed thickening of posterior wall during diastole (PWd) with aging, but middle-aged PAK1$^{-/-}$ female mice showed the thickest wall. **(D)**. Both middle-aged PAK1$^{-/-}$ males and females showed increased left ventricular (LV) mass. **(E)** Relative wall thickness (RWT) increased in old PAK1$^{-/-}$ females. **(F)** Peak myocardial contraction velocity, s', was slower in middle-aged PAK1$^{-/-}$ female hearts. **(G)** Middle-aged PAK1$^{-/-}$ females showed the slowest peak

myocardial relaxation velocity, e'. **(H)** Peak blood inflow velocity E/e' ratio was higher in middle-aged PAK1$^{-/-}$ females. **(I)** E wave deceleration time (DT) was the longest in middle-aged PAK1$^{-/-}$ females. Young: 3–6 months, old: 12–15 months. Males are represented using left bar graphs and females using right bar graphs. Data presented as mean ± SEM, n=6–8. Males and females were analyzed separately with two-way ANOVA Fisher LSD test.

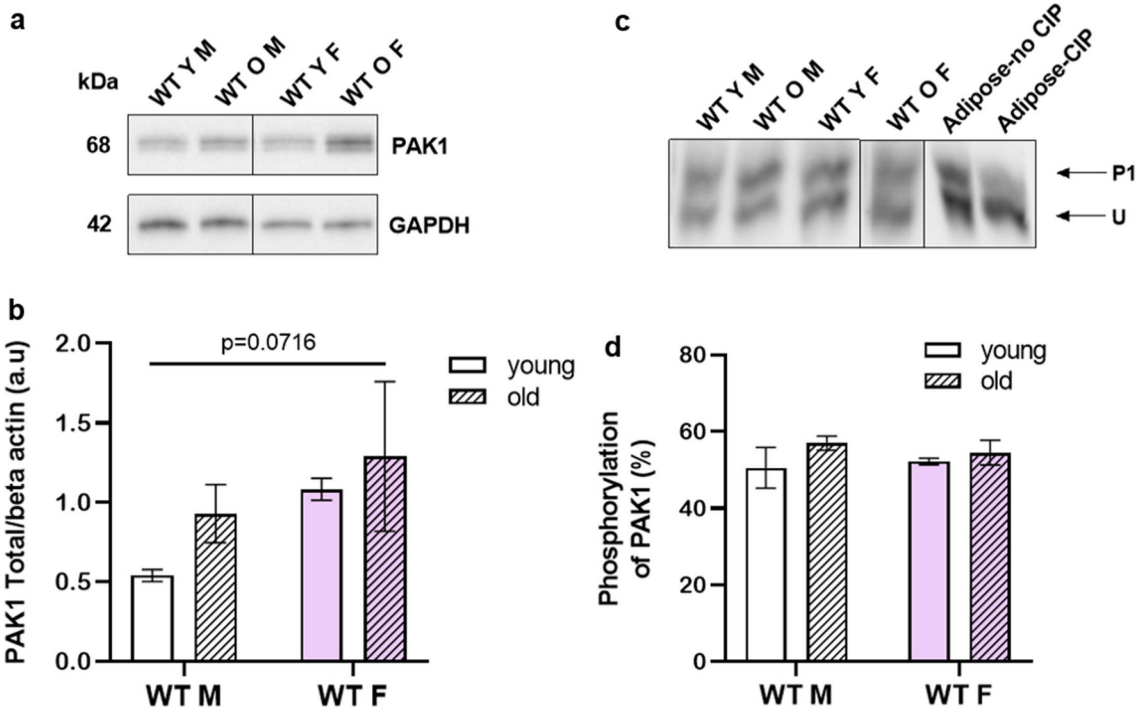

Fig. 5. PAK1 was present in visceral adipose tissue

(A) Total PAK1 abundance and beta-actin as loading control were detected by Western blot on visceral adipose tissue prepared from perigonadal fat depots. **(B)** Quantification of PAK1 over beta-actin showed a trend for increased PAK1 abundance in visceral adipose tissue of older WT female mice. **(C)** PAK1 phosphorvariants were separated on 8% SDS-PAGE phos-tag gel. Bottom band is un-phosphorylated PAK1 and band above is phosphorylated PAK1 with 1 phosphate group. To verify that such band was phosphorylated PAK1, a sample of WT adipose tissue was treated with calf intestine phosphatase (CIP). **(D)** Quantification of PAK1 phosphorylation (p-PAK1 1P/Total PAK1) did not show differences between groups. Young: 3–6 months, old: 12–15 months. Data presented as mean ± SEM. n=3. Data was analyzed using two-way ANOVA Fisher LSD test.

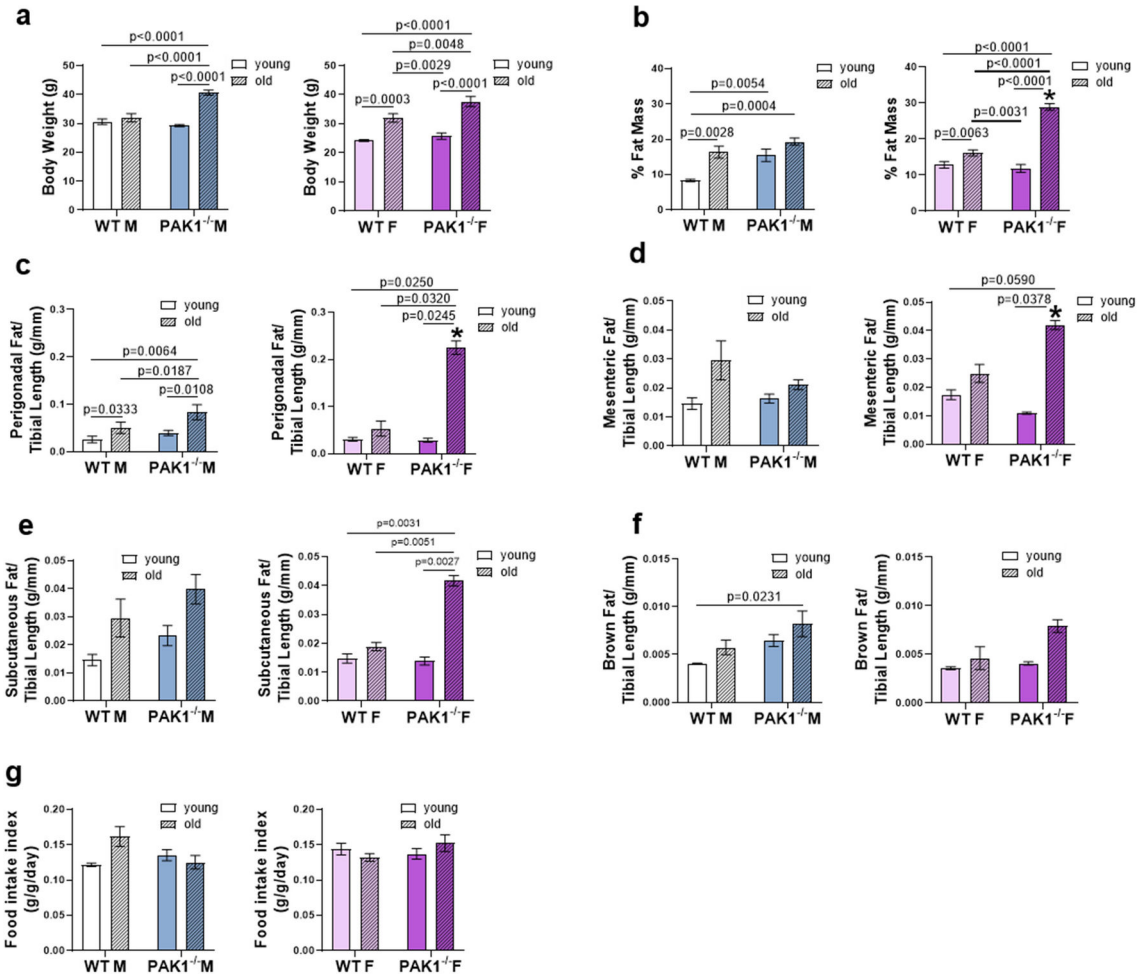

Fig. 6. Middle-aged PAK1$^{-/-}$ females exhibited increased adiposity

(A) Both PAK1$^{-/-}$ males and females exhibited increased body weight (g) with aging. **(B)** Body composition measured as % fat mass/body weight, using Nuclear Magnetic Resonance (NMR), was the highest in middle-aged PAK1$^{-/-}$ female mice. **(C)** Perigonadal fat mass normalized by tibia length (g/mm) was the highest in middle-aged PAK1$^{-/-}$ female mice. **(D)** Mesenteric fat mass normalized by tibia length (g/mm) was highest in middle-aged PAK1$^{-/-}$ female mice. **(E)** Middle-aged PAK1$^{-/-}$ females exhibited the highest subcutaneous fat mass normalized by tibia length (g/mm). **(F)** Brown adipose tissue weight/ tibia length (g/mm) did not differ between groups. **(G)** Food intake index expressed as food intake (g)/ body weight (g) per day, did not differ between groups. Young: 3–6 months, old: 12–15 months. Males are represented using left bar graphs and females using right bar graphs. Data presented as mean ± SEM, n=3–11. Males and females were analyzed separately with two-way ANOVA Fisher LSD test. *p < 0.05 for females vs males according to an independent Student's *t*-test.

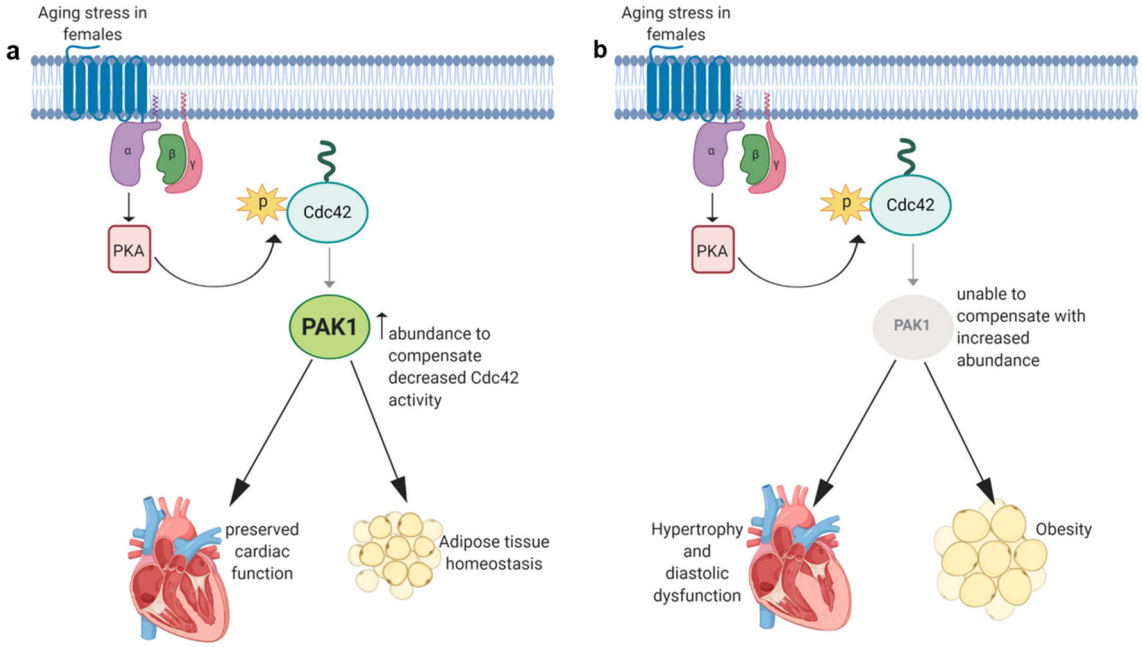

Fig. 7. Scheme illustrating preservation of cardiac function in response to aging in WT female hearts that involves increased PAK1 abundance as a compensatory mechanism to decreased Cdc42 activity. A similar mechanism may preserve adipose tissue homeostasis in middle-aged females

(A) Aging in females may promote GPCR (G-protein-coupled receptors) activation and PKA activation with the consequent phosphorylation and inactivation of Cdc42. Phosphorylation of Cdc42 promotes its interaction with GDI (guanine nucleotide dissociation inhibitor) forming inactive complexes that translocate from the plasma membrane to the cytosol. As a compensatory mechanism, middle-aged female may increase PAK1 abundance in cardiac and adipose tissue. We propose that this occurs to preserve cardiac function and adipose tissue homeostasis in females during aging. **(B)** Under pathological conditions, in which aged females are not able to respond with increased PAK1 abundance, or as a consequence of PAK1 deletion as in our PAK1$^{-/-}$ aged female mice, cardiac dysfunction and obesity are observed. Created with BioRender.com.